Title: Climatic controls of decomposition drive the global biogeography of forest tree symbioses

Authors: *Steidinger BS[1]*, Crowther TW[2]†*, Liang J†[3,4]*, Van Nuland ME[1], Werner GDA[5], Reich PB[6,7], Nabuurs G[8], de-Miguel S[9,10], Zhou M[3], Picard N[11], Herault B[12], Zhao X[4], Zhang C[4], Routh D[2], [GFBi Author List], and Peay KG[1]†*

Affiliations:
[1] Department of Biology, Stanford University, Stanford CA USA
[2] Department of Environmental Systems Science, ETH Zürich, Zürich, Switzerland
[3] Department of Forestry and Natural Resources, Purdue University, West Lafayette, IN, USA
[4] Research Center of Forest Management Engineering of State Forestry Administration, Beijing Forestry University, Beijing, China
[5] Department of Zoology, University of Oxford, Oxford UK
[6] Department of Forest Resources, University of Minnesota
[7] Hawkesbury Institute for the Environment, Western Sydney University
[8] Wageningen University and Research
[9] Departament de Producció Vegetal i Ciència Forestal, Universitat de Lleida-Agrotecnio Center
[10] Forest Science and Technology Centre of Catalonia (CTFC)
[11] Food and Agriculture Organization of the United Nations
[12] Cirad, INP-HB, Univ Montpellier, UPR Forêts et Sociétés

*These authors contributed equally to this work and share the first-author
†Corresponding authors: Email kpeay@stanford.edu; albeca.liang@gmail.com; tom.crowther@usys.ethz.ch

GFBi Author List

Meinrad Abegg [1], Yves Adou Yao [2], Giorgio Alberti [3], Angelica Almeyda Zambrano [4], Esteban Alvarez-Davila [5], Patricia Alvarez-Loayza [6], Luciana F. Alves [7], Christian Ammer [8], Clara Antón-Fernández [9], Alejandro Araujo-Murakami [10], Luzmila Arroyo [11], Valerio Avitabile [12], Gerardo Aymard [13], Timothy Baker [14], Radomir Bałazy[15], Olaf Banki [16], Jorcely Barroso [17], Meredith Bastian [18], Jean-Francois Bastin [19], Luca Birigazzi [20], Philippe Birnbaum [21], Robert Bitariho [22], Pascal Boeckx [23], Frans Bongers [24], Olivier Bouriaud [25], Pedro Brancalion [26], Susanne Brandl [27], Francis Q. Brearley [28], Roel Brienen [29], Eben Broadbent [30], Helge Bruelheide [31], Filippo Bussotti [32], Roberto Cazzolla Gatti [33], Ricardo Cesar [34], Goran Cesljar [35], Robin Chazdon [36], Han Y. H. Chen [37], Chelsea Chisholm [38], Emil Cienciala [39], Connie J. Clark [40], David Clark [41], Gabriel Colletta [42], Richard Condit [43], David Coomes [44], Fernando Cornejo Valverde [45], Jose J. Corral-Rivas [46], Philip Crim [47], Jonathan Cumming [48], Selvadurai Dayanandan [49], André L. de Gasper [50], Mathieu Decuyper [51], Géraldine Derroire [52], Ben DeVries [53], Ilija Djordjevic [54], Amaral Iêda [55], Aurélie Dourdain [56], Nestor Laurier Engone Obiang [57], Brian Enquist [58], Teresa Eyre [59], Adandé Belarmain Fandohan [60], Tom M. Fayle [61], Ted R. Feldpausch [62], Leena Finér [63], Markus Fischer [64], Christine Fletcher [65], Jonas Fridman [66], Lorenzo Frizzera [67], Javier G. P. Gamarra [68], Damiano Gianelle [69], Henry B. Glick

[70], David Harris [71], Andrew Hector [72], Andreas Hemp [73], Geerten Hengeveld [74], John Herbohn [75], Martin Herold [76], Annika Hillers [77], Eurídice N. Honorio Coronado [78], Markus Huber [79], Cang Hui [80], Kook Jo Hyun [81], Thomas Ibanez [82], Bin Jung Il [83], Nobuo Imai [84], Andrzej M. Jagodzinski [85], Bogdan Jaroszewicz [86], Vivian Johannsen [87], Carlos A. Joly [88], Tommaso Jucker [89], Viktor Karminov [90], Kuswata Kartawinata [91], Elizabeth Kearsley [92], David Kenfack [93], Deborah Kennard [94], Sebastian Kepfer-Rojas [95], Gunnar Keppel [96], Mohammed Latif Khan [97], Timothy Killeen [98], Hyun Seok Kim [99], Kanehiro Kitayama [100], Michael Köhl [101], Henn Korjus [102], Florian Kraxner [103], Diana Laarmann [104], Mait Lang [105], Simon Lewis [106], Huicui Lu [107], Natalia Lukina [108], Brian Maitner [109], Yadvinder Malhi [110], Eric Marcon [111], Beatriz Marimon [112], Ben Hur Marimon-Junior [113], Andrew Robert Marshall [114], Emanuel Martin [115], Olga Martynenko [116], Jorge A. Meave [117], Omar Melo-Cruz [118], Casimiro Mendoza [119], Cory Merow [120], Abel Monteagudo Mendoza [121], Vanessa Moreno [122], Sharif A. Mukul [123], Philip Mundhenk [124], Maria G. Nava-Miranda [125], David Neill [126], Victor Neldner [127], Radovan Nevenic [128], Michael Ngugi [129], Pascal Niklaus [130], Jacek Oleksyn [131], Petr Ontikov [132], Edgar Ortiz-Malavasi [133], Yude Pan [134], Alain Paquette [135], Alexander Parada Gutierrez [136], Elena Parfenova [137], Minjee Park [138], Marc Parren [139], Narayanaswamy Parthasarathy [140], Pablo L. Peri [141], Sebastian Pfautsch [142], Oliver Phillips [143], Maria Teresa Piedade [144], Daniel Piotto [145], Nigel C. A. Pitman [146], Irina Polo [147], Lourens Poorter [148], Axel Dalberg Poulsen [149], John R. Poulsen [150], Hans Pretzsch [151], Freddy Ramirez Arevalo [152], Zorayda Restrepo-Correa [153], Mirco Rodeghiero [154], Samir Rolim [155], Anand Roopsind [156], Francesco Rovero [157], Ervan Rutishauser [158], Purabi Saikia [159], Philippe Saner [160], Peter Schall [161], Mart-Jan Schelhaas [162], Dmitry Schepaschenko [163], Michael Scherer-Lorenzen [164], Bernhard Schmid [165], Jochen Schöngart [166], Eric Searle [167], Vladimír Seben [168], Josep M. Serra-Diaz [169], Anatoly Shvidenko [170], Javier Silva-Espejo [171], Marcos Silveira [172], James Singh [173], Plinio Sist [174], Ferry Slik [175], Bonaventure Sonké [176], Alexandre F. Souza [177], Krzysztof Stereńczak [178], Jens-Christian Svenning [179], Miroslav Svoboda [180], Natalia Targhetta [181], Nadja Tchebakova [182], Hans ter Steege [183], Raquel Thomas [184], Elena Tikhonova [185], Peter Umunay [186], Vladimir Usoltsev [187], Fernando Valladares [188], Fons van der Plas [189], Tran Van Do [190], Rodolfo Vasquez Martinez [191], Hans Verbeeck [192], Helder Viana [193], Simone Vieira [194], Klaus von Gadow [195], Hua-Feng Wang [196], James Watson [197], Bertil Westerlund [198], Susan Wiser [199], Florian Wittmann [200], Verginia Wortel [201], Roderick Zagt [202], Tomasz Zawila-Niedzwiecki [203], Zhi-Xin Zhu [204], Irie Casimir Zo-Bi [205]

GFBi Author Affiliations

[1] WSL Swiss Federal Institute for Forest, Snow and Landscape Research, Birmensdorf, Switzerland
[2] UFR Biosciences, University Félix Houphouët-Boigny, Côte d'Ivoire
[3] Department of Agricultural, Food, Environmental and Animal Sciences, University of Udine, 33100 Udine, Italy; Istitute of Biometeorology, National Research Council (CNR-IBIMET), 50145 Firenze, Italy
[4] Spatial Ecology and Conservation Lab, Department of Tourism, Recreation and Sport Management, University of Florida, Gainesville, Florida, 32611 USA

[5] Universidad Nacional Abierta y a Distancia, UNAD; Fundacion ConVida, Medellin, Colombia
[6] Field Museum of Natural History, 1400 Lake Shore Drive, Chicago, IL 60605, USA,
[7] Center for Tropical Research, Institute of the Environment and Sustainability, UCLA, USA
[8] Silviculture and Forest Ecology of the Temperate Zones, University of Göttingen, Germany
[9] Division of Forest and Forest Resources. Norwegian Institute of Bioeconomy Research (NIBIO), Norway
[10] Museo de Historia Natural Noel Kempff Mercado, Universidad Autonoma Gabriel Rene Moreno, Santa Cruz de la Sierra, Bolivia
[11] Museo de Historia Natural Noel Kempff Mercado, Universidad Autonoma Gabriel Rene Moreno, Santa Cruz de la Sierra, Bolivia
[12] European Commission, Joint Research Centre, Ispra, Italy; Wageningen University & Research, Netherlands
[13] UNELLEZ-Guanare, Programa de Ciencias del Agro y el Mar, Herbario Universitario (PORT), Portuguesa 3323, Venezuela
[14] School of Geography, University of Leeds, UK
[15] Department of Geomatics, Forest Research Institute, Braci Leśnej 3 Street, Sękocin Stary, 05-090 Raszyn, Poland
[16] Naturalis Biodiversity Centre, Darwinweg 2, 2333 CR Leiden, Netherlands
[17] Universidade Federal do Acre, Campus Floresta, Cruzeiro do Sul, Acre, Brazil
[18] Smithsonian's National Zoo, 3001 Connecticut Ave NW, Washington, DC 20008, USA
[19] Institute of Integrative Biology, ETH Zurich, Univeritätstrasse 16, 8092, Switzerland
[20] Food and Agriculture Organization of the United Nations, Rome, Italy
[21] Centre de coopération internationale en recherche agronomique pour le développement, France
[22] Institute of Tropical Forest Conservation, Mbarara University of Sciences and Technology, Mbarara, Uganda
[23] Ghent University, Isotope Bioscience Laboratory - ISOFYS, Coupure Links 653, 9000 Gent, Belgium
[24] Wageningen University & Research, PO Box 47, 6700AA Wageningen, Netherlands
[25] Stefan cel Mare University of Suceava, Strada Universității 13, Suceava 720229, Romania
[26] Department of Forest Sciences, Luiz de Queiroz College of Agriculture, University of São Paulo, Piracicaba, SP 13418-900, Brazil
[27] Bavarian State Institute of Forestry, Hans-Carl-von-Carlowitz-Platz 1, Freising 85354, Germany
[28] Manchester Metropolitan University, UK
[29] School of Geography, University of Leeds, UK
[30] Spatial Ecology and Conservation Lab, School of Forest Resources and Conservation, University of Florida, Gainesville, Florida, 32611 USA
[31] Institute of Biology Geobotany and Botanical Garden, Martin Luther University Halle-Wittenberg & German Centre for Integrative Biodiversity Research (iDiv) Halle-Jena-Leipzig, Germany
[32] University of Firenze. Department of Agriculture, Food, Environment and Forest (DAGRI). Piazzale delle Cascine 28, 50144 Firenze. Italy
[33] Biological Institute, Tomsk State University, Tomsk, 634050 Russia; Department of Forestry and Natural Resources, Purdue University, West Lafayette, Indiana, 47907 USA

[34] Department of Forest Sciences, Luiz de Queiroz College of Agriculture, University of São Paulo, Piracicaba, SP 13418-900. Brazil
[35] Department of Spatial regulation, GIS and Forest Policy, Institute of Forestry, Kneza Višeslava 3, 11030 Beograd, Srbija
[36] University of Connecticut, Department of Ecology and Evolutionary Biology, Storrs, CT 06268-3043 USA; University of the Sunshine Coast, Tropical Forests and People Research Centre, Maroochydore, Queensland, Australia
[37] Faculty of Natural Resources Management, Lakehead University, Thunder Bay, Ontario, Canada, P7B 5E1; Key Laboratory for Humid Subtropical Eco-Geographical Processes of the Ministry of Education, Fujian Normal University, Fuzhou, China, 350007
[38] Center for Macroecology, Evolution and Climate, Natural History Museum of Denmark, University of Copenhagen, Universitetsparken 15, 2100 Copenhagen, Denmark
[39] IFER - Institute of Forest Ecosystem Research, Jilove u Prahy; Global Change Research Institute CAS, Brno, Czech Republic
[40] Nicholas School of the Environment, Duke University, NC USA
[41] Department of Biology, University of Missouri-St. Louis, St. Louis, MO USA
[42] Department of Plant BIology, Institute of Biology, University of Campinas, UNICAMP, Brazil
[43] Smithsonian Tropical Research Institute, Apartado 0843-03092, Balboa, Ancon, Panama
[44] Department of Plant Sciences, University of Cambridge, Downing Street, Cambridge, CB2 3EA, UK
[45] Andes to Amazon Biodiversity Program, Madre de Dios, Madre de Dios, Peru
[46] Facultad de Ciencias Forestales, Universidad Juárez del Estado de Durango, Mexico
[47] School of Mathematics and Sciences, The College of Saint Rose, Albany, NY, 12205, USA; Department of Biology, West Virginia University, Morgantown, WV, 26506, USA
[48] Department of Biology, West Virginia University, Morgantown, WV, 26501, USA
[49] Biology Department, Concordia University, L-SP 445-01, Loyola Campus7141, Sherbrooke Street W. Montreal, Quebec, Canada
[50] Natural Science Department, Universidade Regional de Blumenau, Brazil
[51] Laboratory of Geo-Information Science and Remote Sensing, Wageningen University & Research; Forest Ecology and Forest Management Group, Wageningen University & Research, Netherlands
[52] Cirad, UMR EcoFoG (AgroParistech, CNRS, Inra, Université des Antilles, Université de la Guyane), Campus Agronomique, Kourou, French Guiana
[53] Department of Geographical Sciences, University of Maryland, USA
[54] Institute of Forestry, Serbia
[55] National Institut Research Amazon, Brazil
[56] Cirad, UMR EcoFoG (AgroParistech, CNRS, Inra, Université des Antilles, Université de la Guyane), Campus Agronomique, Kourou, French Guiana
[57] IRET, Herbier National du Gabon (CENAREST), Libreville, Gabon
[58] Department of Ecology and Evolutionary Biology, University of Arizona, Tucson, AZ, 85719, USA; The Santa Fe Institute, Santa Fe, New Mexico, 87501, USA
[59] Queensland Herbarium, Department of Environment and Science, Australia
[60] Ecole de Foresterie et Ingénierie du Bois, Université Nationale d'Agriculture, Bénin
[61] Biology Centre of the Czech Academy of Sciences, Institute of Entomology, Branisovska 31, 370 05 Ceske Budejovice, Czech Republic

[62] Geography, College of Life and Environmental Sciences, University of Exeter, Exeter, UK
[63] Natural Resources Institute, Latokartanonkaari 9 FI-00790, Helsinki, Finland
[64] Institute of Plant Sciences, University of Bern, Hochschulstrasse 6, 3012 Bern, Switzerland
[65] Forest Research Institute Malaysia, Jalan Frim, Kepong, 52109 Kuala Lumpur, Selangor, Malaysia
[66] Department of Forest Resource Management, Swedish University of Agricultural Sciences SLU, Sweden
[67] Department of Sustainable Agro-Ecosystems and Bioresources, Research and Innovation Center, Fondazione Edmund Mach di San Michele all'Adige, Via E. Mach, 1 38010 S. Michele all'Adige (TN), Italy
[68] Food and Agriculture Organization of the United Nations, Viale delle Terme di Caracalla, 00153 Rome, Italy
[69] Department of Sustainable Agro-Ecosystems and Bioresources, Research and Innovation Center, Fondazione Edmund Mach di San Michele all'Adige, Via E. Mach, 1 38010 S. Michele all'Adige (TN), Italy
[70] Yale University, School of Forestry and Environmental Studies, CT, USA
[71] Royal Botanic Garden Edinburgh, 20A Inverleith Row, Edinburgh EH3 5LR, Scotland, UK
[72] University of Oxford, Department of Plant Sciences, OX1 3RB, Oxford, UK
[73] University of Bayreuth, Department of Plant Systematics, Universitätsstrasse 30, 95447 Bayreuth, Germany
[74] Wageningen Univeristy and Research, 6708 PB Wageningen, Netherlands
[75] Tropical Forests and Peopel Research Centre, University of the Sunshine Coast, Maroochydore DC, Queensland 4558, Australia
[76] Laboratory for Geoinformation Science and Remote Sensing, Wageningen University, 6708 PB Wageningen, Netherlands
[77] The Royal Society for the Protection of Birds, Sandy, UK
[78] Instituto de Investigaciones de la Amazonía Peruana, Av. José Abelardo Quiñones km 2.5, Iquitos, Peru
[79] WSL Swiss Federal Institute for Forest, Snow and Landscape Research, Switzerland
[80] Centre for Invasion Biology, Department of Mathematical Sciences, Stellenbosch University, Matieland 7602, South Africa;Theoretical Ecology Unit, African Institute for Mathematical Sciences, Cape Town 7945, South Africa
[81] Forest Resources Information Division, Korea Forest Promotion Institute, South Korea
[82] Institut Agronomique néo-Calédonien (IAC), Equipe Sol & Végétation (SolVeg), BPA5, 98800 Nouméa, New Caledonia
[83] Forest Resources Information Division, Korea Forest Promotion Institute, South Korea
[84] Department of Forest Science, Tokyo University of Agriculture, Japan
[85] Institute of Dendrology, Polish Academy of Sciences, Parkowa 5, 62-035 Kórnik, Poland; Poznań University of Life Sciences, Department of Game Management and Forest Protection, Wojska Polskiego 71c, 60-625 Poznań, Poland
[86 Bialowieza Geobotanical Station, Faculty of Biology, University of Warsaw, Sportowa 19, 17-230 Białowieża, Poland
[87] Department of Geosciences and Natural Resource Management, University of Copenhagen, Nørregade 10, 1165 København, Denmark
[88] Plant Biology Department, Biology Institute, State University of Campinas, UNICAMP, Campinas, SP, 13083-862, Brazil [ORCID # 0000-0002-7945-2805]

[89] CSIRO Land and Water, Centre for Environment and Life Sciences, Floreat, WA, 6014 Australia
[90] Bauman Moscow State Technical University, Russia
[91] Integrative Research Center, the Field Museum of Natural History, 1400 Lake Shore Drive, Chicago, IL 60605, USA
[92] Centre for the Research and Technology of Agro-Environmental and Biological Sciences, CITAB; University of Trás-os-Montes and Alto Douro, UTAD; Escola Superior Agrária de Viseu, Portugal
[93] CTFS-ForestGEO, Smithsonian Tropical Research Institute, Apartado 0843-03092, Balboa, Ancon, Panama
[94] Department of Physical and Environmental Sciences, Colorado Mesa University, 1100 North Ave, Grand Junction, CO 81501, USA
[95] Department of Geosciences and Natural Resource Management, University of Copenhagen, Nørregade 10, 1165 København, Denmark
[96] School of Natural and Built Environments and Future Industries Institute, University of South Australia, GPO Box 2471, Adelaide, SA 5001
[97] Department of Botany, Dr. Harisingh Gour Central University, Sagar - 470003, MP, India
[98] Museo de Historia Natural Noel Kempff Mercado, Universidad Autonoma Gabriel Rene Moreno, Santa Cruz de la Sierra, Bolivia
[99] Department of Forest Sciences, Seoul National University, Seoul 08826, Republic of Korea; Interdisciplinary Program in Agricultural and Forest Meteorology, Seoul National University, Seoul 08826, Republic of Korea; National Center for Agro Meteorology, Seoul 08826, Republic of Korea; Research Institute for Agriculture and Life Sciences, Seoul National University, Seoul 08826, Republic of Korea
[100] Graduate School of Agriculture, Kyoto University, Yoshidahonmachi, Sakyo Ward, Kyoto, Kyoto Prefecture 606-8501, Japan
[101] Institute for World Forestry, University of Hamburg, Mittelweg 177 20148 Hamburg Germany
[102] Institute of Forestry and Rural Engineering, Estonian University of Life Sciences, Friedrich Reinhold Kreutzwaldi 1, 51014 Tartu, Estonia
[103] International Institute for Applied Systems Analysis, Laxenburg, Austria
[104] Institute of Forestry and Rural Engineering, Estonian University of Life Sciences, Friedrich Reinhold Kreutzwaldi 1, 51014 Tartu, Estonia
[105] Institute of Forestry and Rural Engineering, Estonian University of Life Sciences, Friedrich Reinhold Kreutzwaldi 1, 51014 Tartu, Estonia
[106] School of Geography University of Leeds, UK; Department of Geography, University College London, UK
[107] Faculty of Forestry, Qingdao Agricultural University, 700 Changcheng Rd, Chengyang Qu, Qingdao Shi, Shandong Sheng, China
[108] Center for Forest Ecology and Productivity RAS, ul. Profsoyuznaya 84, 32, Russia
[109] Department of Ecology and Evolutionary Biology, University of Arizona, Tucson, AZ, 85719, USA
[110] School of Geography, University of Oxford, UK
[111] UMR EcoFoG, AgroParisTech, CNRS, Cirad, INRA, Université des Antilles, Université de Guyane, French Guiana

[112] Departamento de Ciências Biológicas, Universidade do Estado de Mato Grosso, Nova Xavantina, Brazil
[113] Departamento de Ciências Biológicas, Universidade do Estado de Mato Grosso, Nova Xavantina, Brazil
[114] Tropical Forests and People Research Centre, University of the Sunshine Coast, Queensland, Australia; Department of Environment & Geography, University of York, UK; Flamingo Land Ltd., North Yorkshire, UK
[115] Department of Wildlife Management, College of African Wildlife Management, Mweka, Tanzania
[116] Forestry Faculty, Bauman Moscow State Technical University, 2-Ya Baumanskaya Ulitsa, д.5, стр.1, Moskva 105005, Russia
[117] Departamento de Ecología y Recursos Naturales, Facultad de Ciencias, Universidad Nacional Autónoma de México, Mexico
[118] Universidad del Tolima, Ibagué, Colombia
[119] Colegio de Profesionales Forestales de Cochabamba, Cochabamba, Bolivia
[120] Ecology and Evolutionary Biology, University of Connecticut, Storrs 06269, CT, USA
[121] Jardín Botánico de Missouri, Oxapampa, Peru, Universidad Nacional de San Antonio Abad del Cusco, Peru
[122] Department of Forest Sciences, Luiz de Queiroz College of Agriculture, University of São Paulo, Piracicaba, SP 13418-900. Brazil
[123] Department of Enviornmental Management, School of Environmental Science and Management, Independent University Bangladesh, Dhaka 1229, Bangladesh; Tropical Forests and People Research Centre, University of the Sunshine Coast, Maroochydore DC, Queensland 4558, Australia
[124] Institute for World Forestry, University of Hamburg, Germany
[125] Instituto de Silvicultura e Industria de la Madera, Universidad Juárez del Estado de Durango, Mexico
[126] Universidad Estatal Amazónica, Puyo, Pastaza, Ecuador
[127] Department of Environment and Science, Queensland Herbarium, Mount Coot Tha Rd, Toowong QLD 4066, Australia
[128] Institute of Forestry Belgrade, Serbia
[129] Department of Environment and Science, Queensland Herbarium, Mount Coot Tha Rd, Toowong QLD 4066, Australia
[130] Department of Evolutionary Biology and Environmental Studies, University of Zurich, Winterthurerstrasse 190, CH-8057 Zurich, Switzerland
[131] Polish Academy of Sciences, Institute of Dendrology, Parkowa 5, PL-62-035 Kórnik, Poland; Department of Forest Resources, University of Minnesota, St. Paul, MN, USA
[132] Bauman Moscow State Technical University, 2-Ya Baumanskaya Ulitsa, д.5, стр.1, Moskva 105005, Russia
[133] Forestry School. Instituto Tecnologico de Costa Rica. Cartago P.O. 159-7050, Costa Rica
[134] USDA Forest Service, USA
[135] Université du Québec à Montréal, Département des sciences biologiques and Centre for Forest Research, PO Box 8888, Centre-ville Station, Montréal, Qc, Canada H3C 3P8
[136] Museo de Historia Natural Noel Kempff Mercado, Universidad Autonoma Gabriel Rene Moreno, Santa Cruz de la Sierra, Bolivia
[137] V.N.Sukachev Institute of Forest of FRC KSC SB RAS, Russia

[138] Department of Forest Sciences, Seoul National University, Seoul 08826, Republic of Korea; Urban Forests Research Center, National Institute of Forest Science, Seoul 02455, Republic of Korea
[139] Wageningen University and Research, 6708 PB Wageningen, Netherlands
[140] Department of Ecology and Environmental Sciences, Pondicherry University, India
[141] Instituto Nacional de Tecnología Agropecuaria (INTA), Universidad Nacional de la Patagonia Austral (UNPA), Consejo Nacional de Investigaciones Científicas y Tecnicas (CONICET), Argentina
[142] School of Social Sciences and Psychology (Urban Studies), Western Sydney University, Locked Bag 1797, Penrith, NSW 2751, Australia
[143] University of Leeds, School of Geography, U.K.
[144] Instituto Nacional de Pesquisas da Amazônia, Brazil
[145] Laboratório de Dendrologia e Silvicultura Tropical, Centro de Formação em Ciências Agroflorestais, Universidade Federal do Sul da Bahia
[146] Field Museum of Natural History, 1400 Lake Shore Drive, Chicago, IL 60605, USA
[147] Jardín Botánico de Medellín, Cl. 73 #51d14, Medellín, Antioquia, Colombia
[148] Wageningen University and Research, 6708 PB Wageningen, Netherlands
[149] Royal Botanic Garden Edinburgh, Arboretum Pl, Edinburgh EH3 5NZ, UK
[150] Nicholas School of the Environment, Duke University, 9 Circuit Dr, Durham, NC 27710, USA
[151] Chair for Forest Growth and Yield Science, TUM School for Life Sciences, Technical University of Munich, Germany
[152] Universidad Nacional de la Amazonía Peruana, Sargento Lores 385 Iquitos, Loreto, Peru
[153] Corporacion COL-TREE; Facultad de Ingeniera Ambinetal, Universidad de Antioquia, Colombia
[154] Department of Sustainable Agro-Ecosystems and Bioresources, Research and Innovation Center, Fondazione Edmund Mach; Agriculture, Food and Environment Centre (C3A), University of Trento, San Michele all`Adige, Italy.
[155] Colaborador do Laboratório de Dendrologia e Silvicultura Tropical, Centro de Formação em Ciências Agroflorestais, Universidade Federal do Sul da Bahia
[156] Department of Biological Sciences, Boise State University, ID, USA
[157] Tropical Biodiversity Section, MUSE - Museo delle Scienze, Trento, Italy; Department of Biology, University of Florence, Florence, Italy
[158] Smithsonian Tropical Research Institute, Apartado 0843-03092, Balboa, Ancon, Panama
[159] Department of Environmental Sciences, Central University of Jharkhand, Brambe-835205, Ranchi, Jharkhand, India
[160] University of Zurich, Rämistrasse 71, 8006 Zurich, Switzerland
[161] Silviculture and Forest Ecology of the Temperate Zones, University of Göttingen, Germany
[162] Wageningen University and Research, 6708 PB Wageningen, Netherlands
[163] International Institute for Applied Systems Analysis, Laxenburg, Austria
[164] Faculty of Biology, Geobotany, University of Freiburg, Fahnenbergplatz, 79085 Freiburg im Breisgau, Germany
[165] University of Zurich, Rämistrasse 71, 8006 Zurich, Switzerland
[166] Instituto Nacional de Pesquisas da Amazônia, Av. André Araújo 2936, 69067-375 Manaus, Brazil

[167] Faculty of Natural Resources Management, Lakehead University, Thunder Bay, Ontario, P7B 5E1, Canada
[168] National Forest Centre, Forest Research Institute Zvolen, T. G. Masaryka 2175, 22, SK - 960 92, Zvolen
[169] Université de Lorraine, AgroParisTech, Inra, Silva, 54000, Nancy, France; Center for Biodiversity Dynamics in a Changing World (BIOCHANGE), Department of Bioscience, Aarhus University
[170] International Institute for Applied Systems Analysis, Laxenburg, Austria
[171] Departamento de Biología, Universidad de la Serena, Casilla 554, La Serena, Chile
[172] Universidade Federal do Acre, Rio Branco, Brazil
[173] Guyana Forestry Commission, Georgetown, Guiana
[174] CIRAD, UPR Forests&Societies, Univ. Montpellier
[175] Environmental and Live Sciences, Faculty of Science, Universiti Brunei Darussalam, Jalan Tungku Link, Gadong, BE1410, Brunei Darussalam
[176] Plant Systematic and Ecology Laboratory, Department of Biology, University of Yaounde
[177] Departamento de Ecologia, Universidade Federal do Rio Grande do Norte, Natal, Brazil
[178] Department of Geomatics, Forest Research Institute, Braci Leśnej 3 Street, Sękocin Stary, 05-090 Raszyn, Poland
[179] Center for Biodiversity Dynamics in a Changing World (BIOCHANGE), Department of Bioscience, Aarhus University; Section for Ecoinformatics & Biodiversity, Department of Bioscience, Aarhus University
[180] Faculty of Forestry and Wood Sciences, Czech University of Life Sciences Prague, Kamýcká 129, Praha 6 Suchdol 16521, Czech Republic
[181] Instituto Nacional de Pesquisas da Amazônia, Av. André Araújo, 2936 - Petrópolis, Manaus - AM, 69067-375, Brazil
[182] V.N.Sukachev Institute of Forest of FRC KSC SB RAS, 50, Akademgorodok, Krasnoyarsk, 660036, Siberia
[183] Naturalis Biodiversity Center, Leiden, The Netherlands & Systems Ecology, Free University Amsterdam, Netherlands
[184] Iwokrama International Centre for Rainforest Conservation and Development (IIC), Georgetown, Guiana
[185] Center for Forest Ecology and Productivity, Russian Academy of Sciences
[186] School of Forestry and Environmental Studies, Yale University, 195 Prospect St, New Haven, CT 06511, USA
[187] Botanical Garden of Ural Branch of Russian Academy of Sciences, Ural State Forest Engineering University, Ekaterinburg, Russia
[188] Museo Nacional de Ciencias Naturales, Calle de José Gutiérrez Abascal, 2, 28006 Madrid, Spain
[189] Systematic Botany and Functional Biodiversity, Institute of Biology, Leipzig University, Germany
[190] Silviculture Research Institute, Vietnamese Academy of Forest Sciences, Duc Thang, Bac Tu Liem, Hanoi, Vietnam
[191] Jardín Botánico de Missouri, Peru
[192] Ghent University, St. Pietersnieuwstraat 33, 9000 Gent, Belgium

406 [193] Centre for the Research and Technology of Agro-Environmental and Biological Sciences,
407 CITAB, University of Trás-os-Montes and Alto Douro, UTAD, Portugal. Escola Superior Agrária
408 de Viseu.
409 [194] Environmental Studies and Research Center, University of Campinas, Rua dos Flamboyants,
410 155, Campinas, SP 13083-867, Brazil.
411 [195] Extraordinary Professor Department of Forest and Wood Science, University of
412 Stellenbosch, South Africa
413 [196] Key Laboratory of Tropical Biological Resources, Ministry of Education, Hainan
414 University, Haikou, Hainan 570228, China
415 [197] Division of Forestry and Natural Resources, West Virginia University, USA
416 [198] Department of Forest Resource Management, Swedish University of Agricultural Sciences
417 SLU, Sweden
418 [199] Manaaki Whenua -- Landcare Research, Lincoln 7640, New Zealand
419 [200] Department of Wetland Ecology, Institute for Geography and Geoecology, Karlsruhe
420 Institute for Technology, Germany
421 [201] Centre for Agricultural Research in Suriname (CELOS), Suriname
422 [202] Tropenbios International, P.O.Box 232, 6700 AE Wageningen, Netherlands
423 [203] Polish State Forests, Coordination Center for Environmental Projects, Poland
424 [204] Institute of Tropical Agriculture and Forestry, Hainan University, Haikou, Hainan, China
425 [205] Department of Forestry and Environment, National Polytechnic Institute (INP-HB),
426 Yamoussoukro, Côte d'Ivoire
427

428 **Manuscript**

429 **The identity of the dominant microbial symbionts in a forest determines the ability of**
430 **trees to access limiting nutrients from atmospheric or soil pools[1,2], sequester carbon[3,4] and**
431 **withstand the impacts of climate change[1-6]. Characterizing the global distribution of**
432 **symbioses, and identifying the factors that control it, are thus integral to understanding**
433 **present and future forest ecosystem functioning. Here we generate the first spatially explicit**
434 **global map of forest symbiotic status using a database of over 1.1 million forest inventory**
435 **plots with over 28,000 tree species. Our analyses indicate that climatic variables, and in**
436 **particular climatically-controlled variation in decomposition rate, are the primary drivers of**
437 **the global distribution of major symbioses. We estimate that ectomycorrhizal (EM) trees,**
438 **which represent only 2% of all plant species[7], constitute approximately 60% of tree stems on**
439 **Earth. EM symbiosis dominates forests where seasonally cold and dry climates inhibit**

decomposition, and are the predominant symbiosis at high latitudes and elevation. In contrast, arbuscular mycorrhizal (AM) trees dominate aseasonally warm tropical forests and occur with EM trees in temperate biomes where seasonally warm-and-wet climates enhance decomposition. Continental transitions between AM and EM dominated forests occur relatively abruptly along climate driven decomposition gradients, which is likely caused by positive plant-microbe feedbacks. Symbiotic N-fixers, which are insensitive to climatic controls on decomposition compared with mycorrhizal fungi, are most abundant in arid biomes with alkaline soils and high maximum temperatures. The climatically driven global symbiosis gradient we document represents the first spatially-explicit, quantitative understanding of microbial symbioses at the global scale and demonstrates the critical role of microbial mutualisms in shaping the distribution of plant species.

Microbial symbionts strongly influence the functioning of forest ecosystems. They exploit inorganic, organic[2] and/or atmospheric forms of nutrients that enable plant growth[1], determine how trees respond to elevated CO_2[6], regulate the respiratory activity of soil microbes[3,8], and affect plant species diversity by altering the strength of conspecific negative density dependence[9]. Despite growing recognition of the importance of root symbioses for forest functioning[1,6,10] and the potential to integrate symbiotic status into Earth system models that predict functional changes to the terrestrial biosphere[10], we lack spatially-explicit, quantitative maps of the different root symbioses at the global scale. Generating these quantitative maps of tree symbiotic states would link the biogeography of functional traits of belowground microbial symbionts with their 3.1 trillion host trees[11], spread across Earth's forests, woodlands, and savannas.

The dominant guilds of tree root symbionts, arbuscular mycorrhizal (AM) fungi, ectomycorrhizal (EM) fungi, ericoid mycorrhizal (ErM) fungi, and nitrogen (N)-fixing bacteria

463 (N-fixer) are all based on the exchange of plant photosynthate for limiting macronutrients. The
464 AM symbiosis evolved nearly 500 million years ago, with EM, ErM and N-fixer plant taxa
465 evolving multiple times from an AM basal state. Plants that form the AM symbiosis comprise
466 nearly 80% of all terrestrial plant species, and principally rely on AM fungi for enhancing mineral
467 phosphorus (P) uptake[12]. In contrast to AM fungi, EM fungi evolved from multiple lineages of
468 saprotrophic ancestors, and as a result some EM fungi are more capable of mobilizing organic
469 sources of soil nutrients (particularly nitrogen)[2]. Association with EM fungi, but not AM fungi,
470 has been shown to allow trees to accelerate photosynthesis in response to increased atmospheric
471 CO_2 when soil nitrogen (N) is limiting[6] and to inhibit soil respiration by decomposer microbes[3,8].
472 Because increased plant photosynthesis and decreased soil respiration both reduce atmospheric
473 CO_2 concentrations, the EM symbiosis is associated with buffering the Earth's climate against
474 anthropogenic changes.

475 In contrast to mycorrhizal fungi, which extract nutrients from the soil, symbiotic N-fixers
476 (Rhizobia and Actinobacteria) convert atmospheric N_2 to plant-usable forms. Symbiotic N-fixers
477 are responsible for a large fraction of biological soil-N inputs, which can increase N-availability
478 in forests where they are locally abundant[13]. Both N-fixing bacteria and EM fungi often demand
479 more plant photosynthate than does the AM symbiosis[12,14,15]. Because tree growth and
480 reproduction are limited by access to inorganic, organic and atmospheric sources of N, the
481 distribution of root symbioses is likely to reflect both environmental conditions that maximize the
482 cost-benefit ratio of symbiotic exchange as well as physiological constraints on different
483 symbionts.

484 In one of the earliest efforts to understand the functional biogeography of plant root
485 symbioses, Sir David Read[16] categorically classified biomes by their perceived dominant

mycorrhizal type and hypothesized that seasonal climates favor hosts associating with EM fungi due to their ability to compete directly for organic N. In contrast, it has been proposed that sensitivity to low temperatures has prevented N-fixers from dominating outside the tropics, despite the potential for N-fixation to alleviate N-limitation in boreal forests[15,17]. However, global scale tests of these proposed biogeographic patterns and their climate drivers are lacking. To address this research gap, we compiled the first global ground-sourced survey database to reveal numerical abundances of each symbiosis across the globe, which is essential for identifying the potential mechanisms underlying transitions in forest symbiotic state along climatic gradients[18,19].

We determined the abundance of tree symbioses using GFBi, an extension from the plot-based Global Forest Biodiversity (GFB) database, which contains over 1.1 million forest inventory plots of individual-based measurement records from which we derive abundance information for entire tree communities (Figure 1). Using published literature on the evolutionary histories of mycorrhizal and N-fixer symbioses, we assigned plant species from the GFBi to one of 5 symbiotic guilds: AM, EM, ErM, N-fixer, and non- or weakly-mycorrhizal (NM). We then used the random forest algorithm with K-fold cross validation to determine the importance and influence of variables related to climate, soil chemistry, vegetation, and topography on the relative abundance of each tree-symbiotic guild (Figure 2). Because decomposition is the dominant process by which soil nutrients become available to plants, we calculated annual and quarterly decomposition coefficients according to the Yasso07 model[20], which describes how temperature and precipitation gradients influence mass-loss rates of different chemical pools of leaf litter (with parameters fit using a previous global study of leaf decomposition, Figures 3, S5). Finally, we projected our predictive models across the globe over the extent global biomes that fell within the multivariate distribution of our model training data (Figures 4, S14-15, see Methods for full description).

509 Our analysis shows that the three most numerically abundant tree symbiotic guilds each
510 have reliable environmental signatures, with the four most important predictors accounting for 81,
511 79, and 52% of the total variability in EM, AM, and N-fixer relative basal area, respectively.
512 Models for ErM and NM lack strong predictive power given the relative rarity of these symbiotic
513 states amongst trees, although the raw data do identify some local abundance hotspots for ErM
514 (Figure S1). As a result, we focus the remainder of results and discussion on the three major tree
515 symbiotic states (EM, AM, N-fixer). Despite the fact that data from N. and S. America constitute
516 65% of the training data (at the 1 by 1 degree grid scale), our models accurately predict the
517 proportional abundances of the three major symbioses across all major geographic regions (Figure
518 S10). The high performance of our models, which is robust to both K-fold cross-validation and
519 rarefying samples so that all continents are represented with equal depth (Figures S11-12), suggest
520 that regional variations in climate (including indirect effects on decomposition) and soil pH (for
521 N-fixers) are the primary factors influencing the relative dominance of each guild at the global
522 scale (geographic origin only explained ~2-5% of the variability in residual relative abundance)
523 (Table S8, Figure S10).

524 Whereas a recent global analysis of root traits concluded that plant evolution has favored
525 reduced dependence on mycorrhizal fungi[21], we find that trees associating with the relatively more
526 C-demanding and recently-derived EM fungi[12,14] represent the dominant tree-symbiosis. By taking
527 the average proportion of EM trees, weighted by spatially-explicit global predictions for tree stem
528 density[11], we estimate that approximately 60% of trees on earth are EM, despite the fact that only
529 2% of plant species associate with EM fungi (vs. 80% associating with AM fungi)[7]. Outside of the
530 tropics, the estimate for EM relative abundance increases to approximately 80% of trees.

Turnover among the major symbiotic guilds results in a tri-modal latitudinal abundance gradient, with the proportion of EM trees increasing (and AM trees decreasing) with distance from the equator, while the upper-quantiles of N-fixing trees reach peak abundance in the arid zone around 30 degrees (Figure 3A, Figure 4). These trends are driven by abrupt transitional regions along continental climatic gradients (Figure 2), which skew the distribution of symbioses among biomes (Figure 3A) and drive strong patterns across geographic and topographic features that influence climate. Moving north or south from the equator, the first transitional zone separates warm (aseasonal), AM-dominated, tropical broadleaf forests (>75% median basal area, vs. 8% for EM trees) from the rest of the EM-dominated world forest system (Figure 2AB; Figure 3A). The transition zone occurs across the globe around 25 degrees N and S latitude, just beyond the dry tropical broadleaf forests (with 25% EM tree basal area; Figure 3A), where average monthly temperature variation reaches 3-5°C (temperature seasonality, Figure 2AB).

Moving further N or S, the second transitional climate zone separates regions where decomposition coefficients during the warmest quarter of the year are less than 2 (see Figure 3B for the associated temperature and precipitation ranges). In N. America and China, this transition zone occurs around 50 degrees N, separating the mixed AM / EM temperate forests from their neighboring EM dominated boreal forests (75 vs 100% EM tree basal area, respectively; Figure 3A). This transitional decomposition zone bypasses W. Europe, which has temperature seasonality > 5°C, but lacks sufficiently wet summers to accelerate decomposition coefficients beyond values associated with mixed AM/EM forests. The latitudinal transitions in symbiotic state observed among biomes are mirrored by within-biome transitions along elevation gradients. For example, in tropical Mexico, warm and wet quarter decomposition coefficients < 2 occur along the slopes of the Sierra Madre, where mixed AM-exclusive and N-fixer woodlands in arid climates transition

554 to EM dominated tropical coniferous forests (75% basal area, Figure 3A, Figure 4ABC, Figure
555 S16-18). The southern hemisphere, which lacks the landmass to support extensive boreal forests,
556 experiences a similar latitudinal transition in decomposition rates along the ecotone separating its
557 tropical and temperate biomes, around 28 degrees S.

558 The abrupt transitions that we detected between forest symbiotic states along
559 environmental gradients suggest that positive feedbacks may exist between climatic and biological
560 controls of decomposition[10,20]. In contrast to AM fungi, some EM fungi can use oxidative enzymes
561 to mineralize organic nutrients from leaf litter, converting nutrients to plant-usable forms[2,5].
562 Relative to AM trees, the leaf litter of EM trees is also chemically more resistant to decomposition,
563 with higher C:N ratios and higher concentrations of decomposition-inhibiting secondary
564 compounds[10]. Thus, EM leaf litter can exacerbate climatic barriers to decomposition, promoting
565 conditions where EM fungi have superior nutrient-acquiring abilities to AM-fungi[5,10]. A recent
566 game theoretical model has shown that positive plant-soil-nutrient feedbacks can lead to local
567 bistability in mycorrhizal symbiosis[22]. Such positive-feedbacks are also known to cause abrupt
568 ecosystem transitions along smooth environmental gradients between woodlands and grasses: trees
569 suppress fires, which promotes seedling recruitment, while grass fuels fires, which kill tree
570 seedlings[23]. The existence of abrupt transitions also suggests that forests in transitional regions
571 along decomposition gradients should be susceptible to drastic turnover in symbiotic state with
572 future environmental changes[23].

573 To illustrate the sensitivity of global patterns of tree symbiosis to climate change, we use
574 the relationships we developed for current climate to project potential changes in forest symbiotic
575 status in the future. Relative to our global predictions using the most recent climate data, model
576 predictions using the projected climates for 2070 suggest the abundance of EM trees will decline

by as much as 10% (using a relative concentration pathway of 8.5 W/m^2; Figure S24). Due to their position along decomposition gradients relative to the abrupt shift from EM to AM forests (Figure 2AB), our models predict the largest declines in EM abundance will occur along the boreal-temperate ecotone, although this model does not estimate the time lags between climate change and forest community responses. The predicted decline in EM trees corroborates the results of common garden transfer and simulated warming experiments, which demonstrate that some important EM hosts will decline at the boreal-temperate ecotone in altered climates[24].

The change in dominant nutrient exchange symbioses along climate gradients highlights the interconnection between atmospheric and soil compartments of the biosphere. The transition from AM to EM dominance corresponds with a shift from P to N limitation of plant growth with increasing latitude[25,26]. Including published global projections of total soil N or P, microbial N, or soil P fractions (labile, occluded, organic, and apatite) did not increase the amount of variation explained by the model or alter the variables identified as most important, and thus were dropped from our analysis. However, our finding that climatic controls of decomposition best predict the dominant mycorrhizal associations mechanistically links symbiont physiology with climatic controls of soil nutrient release from leaf litter. These findings are consistent with Read's hypothesis[16] that slow decomposition at high latitudes favors EM fungi due to their increased capacity to liberate organic nutrients[2]. Thus, while more experiments are necessary to understand the specific mechanism by which nutrient competition favors dominance of AM or EM symbioses[18], we propose that the latitudinal and elevational transitions from AM to EM dominated forests be called Read's Rule.

While our analyses focus on prediction at large spatial scales appropriate to the available data, our findings with respect to Read's Rule also provide insight into how soil factors structure

600 the fine-scale distributions of tree symbioses within our grid cells. For example, while at a coarse
601 scale we find that EM trees are relatively rare in many wet tropical forests, individual tropical sites
602 in our raw data span the full range from 0 – 100 % EM basal area. In much of the wet tropics, these
603 EM dominated sites exist as outliers within a matrix of predominantly AM trees. In an apparent
604 exception that proves Read's Rule, in aseasonal warm neotropical climates, which accelerate leaf-
605 decomposition and promote regional AM dominance (Figure 3), EM dominated tree stands can
606 develop in sites where poor soils and recalcitrant litter slow decomposition and N
607 mineralization[18,27]. Landscape-scale variation in the relative abundance of symbiotic states also
608 changes along climate gradients, with variability highest in xeric and temperate biomes (Figure
609 S3-4), suggesting that the potential of local nutrient variability to favor particular symbioses is
610 contingent on climate.

611 Whereas EM trees are associated with ecosystems where plant growth is thought to be
612 primarily N-limited, N-fixer trees are not. Our results highlight the global extent of the "N-cycling
613 paradox," wherein some metrics suggest that N-limitation is greater in the temperate zone[25,26], yet
614 N-fixing trees are relatively more common in the tropics[15,28] (Figure 3A). We find that N-fixers,
615 which we estimate represent 7% of all trees, dominate forests with annual max temperatures >35°C
616 and alkaline soils (particularly in North America and Africa, Figure 2C). They have the highest
617 relative abundance in xeric shrublands (24%), tropical savannas (21%), and dry broadleaf forest
618 biomes (20%), but are nearly absent from boreal forests (<1%) (Figure 3A, Figure 4). The decline
619 in N-fixer tree abundance we observed with increasing latitude is also associated with a previously
620 documented latitudinal shift in the identity of N-fixing microbes, from facultative N-fixing
621 rhizobial bacteria in tropical forests to obligate N-fixing actinorhizal bacteria in temperate
622 forests[28]. Our data are not capable of fully disentangling the several hypotheses that have been

623 proposed to reconcile the N-cycling paradox[15]. However, our results are consistent with the model
624 prediction[17] and regional empirical evidence[19,29,30] that N-fixing trees are particularly important in
625 arid biomes. Based primarily on the observed positive, nonlinear association of N-fixer relative
626 abundance with the mean temperature of the hottest month (Figure 2C), our models predict a two-
627 fold increase in N-fixer relative abundance when transitioning from humid to dry tropical forest
628 biomes (Figure 3A).

629 Although soil microbes are a dominant component of forests, both in terms of diversity and
630 ecosystem functioning[5,6,10], identifying global-scale microbial biogeographic patterns remains an
631 ongoing research priority. Our analyses confirm that Read's Rule, which is one of the first
632 proposed biogeographic rules specific to microbial symbioses, successfully describes global
633 transitions between mycorrhizal guilds. More generally, climate driven turnover among the major
634 plant-microbe symbioses represents a fundamental biological pattern in the Earth system, as forests
635 transition from low-latitude arbuscular mycorrhizal, to N-fixer, to high-latitude ectomycorrhizal
636 ecosystems. The predictions of our model (which we make available as a global raster layer) can
637 now be used to represent these critical ecosystem variations in global biogeochemical models used
638 to predict climate-biogeochemical feedbacks within and between trees, soils, and the atmosphere.
639 Additionally, the layer containing the proportion of N-fixing trees can be used to map potential
640 symbiotic N-fixation, which links together atmospheric pools of C and N. Future work can extend
641 our findings to incorporate multiple plant growth forms and non-forested biomes, where similar
642 patterns likely exist, to generate a complete global perspective. Our predictive maps leverage the
643 most comprehensive global forest dataset to generate the first quantitative global map of forest tree
644 symbioses, demonstrating how nutritional mutualisms are coupled with the global distribution of
645 plant communities.

References

1 Batterman, S. A. *et al.* Key role of symbiotic dinitrogen fixation in tropical forest secondary succession. *Nature* **502**, 224-227, doi:10.1038/nature12525 (2013).

2 Shah, F. *et al.* Ectomycorrhizal fungi decompose soil organic matter using oxidative mechanisms adapted from saprotrophic ancestors. *New Phytol* **209**, 1705-1719, doi:10.1111/nph.13722 (2016).

3 Averill, C., Turner, B. L. & Finzi, A. C. Mycorrhiza-mediated competition between plants and decomposers drives soil carbon storage. *Nature* **505**, 543-+, doi:10.1038/nature12901 (2014).

4 Clemmensen, K. E. *et al.* Roots and associated fungi drive long-term carbon sequestration in boreal forest. *Science* **339**, 1615-1618, doi:10.1126/science.1231923 (2013).

5 Cheeke, T. E. *et al.* Dominant mycorrhizal association of trees alters carbon and nutrient cycling by selecting for microbial groups with distinct enzyme function. *New Phytol.* **214**, 432-442, doi:10.1111/nph.14343 (2017).

6 Terrer, C., Vicca, S., Hungate, B. A., Phillips, R. P. & Prentice, I. C. Mycorrhizal association as a primary control of the CO2 fertilization effect. *Science* **353**, 72-74, doi:10.1126/science.aaf4610 (2016).

7 Brundrett, M. C. in *Biogeography of Mycorrhizal Symbiosis* 533-556 (Springer, 2017).

8 Averill, C. & Hawkes, C. V. Ectomycorrhizal fungi slow soil carbon cycling. *Ecol Lett* **19**, 937-947, doi:10.1111/ele.12631 (2016).

9 Bennett, J. A. *et al.* Plant-soil feedbacks and mycorrhizal type influence temperate forest population dynamics. *Science* **355**, 181-184 (2017).

10 Phillips, R. P., Brzostek, E. & Midgley, M. G. The mycorrhizal-associated nutrient economy: a new framework for predicting carbon-nutrient couplings in temperate forests. *New Phytol.* **199**, 41-51, doi:10.1111/nph.12221 (2013).

11 Crowther, T. W. *et al.* Mapping tree density at a global scale. *Nature* **525**, 201 (2015).

12 Heijden, M. G., Martin, F. M., Selosse, M. A. & Sanders, I. R. Mycorrhizal ecology and evolution: the past, the present, and the future. *New Phytol.* **205**, 1406-1423 (2015).

13 Binkley, D., Sollins, P., Bell, R., Sachs, D. & Myrold, D. Biogeochemistry of adjacent conifer and alder-conifer stands. *Ecology* **73**, 2022-2033 (1992).

14 Leake, J. *et al.* Networks of power and influence: the role of mycorrhizal mycelium in controlling plant communities and agroecosystem functioning. *Canadian Journal of Botany* **82**, 1016-1045 (2004).

15 Hedin, L. O., Brookshire, E. N. J., Menge, D. N. L. & Barron, A. R. in *Annual Review of Ecology Evolution and Systematics* Vol. 40 *Annual Review of Ecology Evolution and Systematics* 613-635 (Annual Reviews, 2009).

16 Read, D. J. Mycorrhizas in Ecosystems. *Experientia* **47**, 376-391, doi:Doi 10.1007/Bf01972080 (1991).

17 Houlton, B. Z., Wang, Y.-P., Vitousek, P. M. & Field, C. B. A unifying framework for dinitrogen fixation in the terrestrial biosphere. *Nature* **454**, 327 (2008).

18 Peay, K. G. The mutualistic niche: mycorrhizal symbiosis and community dynamics. *Annual Review of Ecology, Evolution, and Systematics* **47**, 143-164 (2016).

19 Pellegrini, A. F., Staver, A. C., Hedin, L. O., Charles-Dominique, T. & Tourgee, A. Aridity, not fire, favors nitrogen-fixing plants across tropical savanna and forest biomes. *Ecology* **97**, 2177-2183 (2016).
20 Tuomi, M. *et al.* Leaf litter decomposition—estimates of global variability based on Yasso07 model. *Ecological Modelling* **220**, 3362-3371 (2009).
21 Ma, Z. *et al.* Evolutionary history resolves global organization of root functional traits. *Nature* (2018).
22 Lu, M. & Hedin, L. O. Global plant–symbiont organization and emergence of biogeochemical cycles resolved by evolution-based trait modelling. *Nature ecology & evolution*, 1 (2019).
23 Scheffer, M., Carpenter, S., Foley, J. A., Folke, C. & Walker, B. Catastrophic shifts in ecosystems. *Nature* **413**, 591 (2001).
24 Reich, P. B. *et al.* Geographic range predicts photosynthetic and growth response to warming in co-occurring tree species. *Nature Climate Change* **5**, 148 (2015).
25 McGroddy, M. E., Daufresne, T. & Hedin, L. O. Scaling of C: N: P stoichiometry in forests worldwide: Implications of terrestrial redfield-type ratios. *Ecology* **85**, 2390-2401 (2004).
26 Reich, P. B. & Oleksyn, J. Global patterns of plant leaf N and P in relation to temperature and latitude. *Proceedings of the National Academy of Sciences of the United States of America* **101**, 11001-11006 (2004).
27 Corrales, A., Mangan, S. A., Turner, B. L. & Dalling, J. W. An ectomycorrhizal nitrogen economy facilitates monodominance in a neotropical forest. *Ecol Lett* **19**, 383-392, doi:10.1111/ele.12570 (2016).
28 Menge, D. N., Lichstein, J. W. & Ángeles-Pérez, G. Nitrogen fixation strategies can explain the latitudinal shift in nitrogen-fixing tree abundance. *Ecology* **95**, 2236-2245 (2014).
29 Liao, W., Menge, D. N., Lichstein, J. W. & Ángeles-Pérez, G. Global climate change will increase the abundance of symbiotic nitrogen-fixing trees in much of North America. *Global Change Biol* (2017).
30 Gei, M. *et al.* Legume abundance along successional and rainfall gradients in Neotropical forests. *Nature ecology & evolution*, 1 (2018).

Figure Legends

Figure 1. The global distribution of GFBi training data. The global map has n=2,768 grid cells at a 1 x 1 degree latitude/longitude resolution. Cells are colored in the red, green and blue spectrum according to the % of total tree basal area occupied by N-fixer, AM, and EM tree symbiotic guilds, as indicated by the ternary plot. Grey cells show the global distribution of forests where we make model projections.

Figure 2. A small number of environmental variables predict the majority of global turnover in forest symbiotic status. Panels show the partial feature contrbutions of different environmental variables on forest symbiotic state. Each row plots the shape of the contribution of the four most important predictors of the proportion of tree basal area belonging to the (a) ectomycorrhizal (EM), (b) arbuscular mycorrhizal (AM), and (c) N-fixer symbiotic guilds (n=2,768). Variables are listed in declining importance from left to right, as determined by inc node purity, with points colored with a red-green-blue gradient according to their position on the x-axis of the most important variable (left-most panels for each guild), allowing cross visualization between predictors. Each panel lists two measures of variable importance, inc node purity (used for sorting) and %IncMSE (see Supplemental Information for description). The abundance of each symbiont type transitions sharply along climatic gradients, suggesting that sites near the threshold are particularly vulnerable to switching their dominant symbiont guild with climate changes.

Figure 3. The distribution of forest symbiotic status across biomes is related to climatic controls over decomposition. (a) Biome level summaries of the median +/- 1 quartile of the predicted % tree basal area per biome for ectomycorrhizal (EM), arbuscular mycorrhizal (AM), and N-fixer symbiotic guilds (n=100 random samples per biome). (b) The dependency of decomposition coefficients (k, solid and dotted lines) on temperature and precipitation during the warmest quarter with respect to predicted dominance of mycorrhizal symbiosis. The transition from AM forests to EM forests between k=1 and 2 is abrupt, which is consistent with positive feedback between climatic and biological controls of decomposition.

Figure 4. Global maps of predicted forest tree symbiotic state. Maps (left) and latitudinal gradients (right, with solid line indicating the median and colored ribbon spanning the range from the 5% and 95% quantiles) of the % of tree basal area for (a) ectomycorrhizal (EM), (b) arbuscular mycorrhizal (AM), and (c) N-fixer symbiotic guilds. All projections are displayed a 0.5 by 0.5 degree lat/long scale with n=28,454.

Acknowledgements

This work was made possible by the Global Forest Biodiversity Database, which represents the work of over 200 independent investigators and their public and private funding agencies (see Supplementary Acknowledgements).

Author Contributions

KGP & TWC conceived the study; TWC, JL, PBR, GN, SdM, MZ, NP, BH, XZ, & CZ conceived and organized the GFBi database; KGP, BSS, GDAW, & MVN compiled the symbiosis database; BSS carried out the primary data analysis; MVN & DR contributed to data compilation and analysis; BSS, TWC, MVN & KGP wrote the initial manuscript; BSS, TWC, JL, MVN, GDAW, PBR, GN, SdM, MZ, NP, BH, XZ, CZ & KGP made substantial revisions to all versions of the manuscript; all other named authors provided forest inventory data and commented on the manuscript.

Data Availability

The GFBi database is available upon written request at https://www.gfbinitiative.org/datarequest. Additionally, the symbiotic state assigned to tree species as a supplementary file, as are global rasters of our model projections for EM, AM, and N-fixer proportion of tree basal area.

Conflict of Interest

The authors declare we have no conflict of interests.

Supplementary Information

For more information on symbiotic guild assignments, model selection, and supplementary analyses, refer to SupplementaryInfo_Steidinger_etal2019.pdf. For the full suite of Supplemental Files, including symbiotic guild assignments and rasters of model projections, refer to SupplementalFiles_Steidinger_etal2019.zip

Methods

We quantified the relative abundance of tree symbiotic guilds across >1.1 million forest census plots combined in the GFBi database, an extension from the plot-based Global Forest Biodiversity (GFB[31]) database. The GFBi database consists of individual-based data that we compiled from all the regional and national GFBi forest inventory data sets. The standardized GFBi data frame, i.e. tree list, comprises tree ID, a unique number assigned to each individual tree; plot ID, a unique string assigned to each plot; plot coordinates, in decimal degrees of WGS84 datum; tree size, in diameter-at-breast-height; trees-per-hectare expansion factor; year of measurement; data set name, a unique number assigned to each forest inventory data set; and binomial scientific tree species names.

We error checked all species names from different forest inventory data sets in three steps. First, we extracted scientific names from original data sets, keeping only the names of genus and species (authority names are removed). Next, we compiled all the species names into five general species lists, one for each continent. Finally, we verified individual species names against 23 online taxonomic databases using the 'taxize' package of R programming language[32]. We assigned each morphospecies a unique name comprising the genus, the string "spp", followed by the data set name and a unique number for that species. For example, "Picea sppCNi1" and "Picea sppCNi2"

797 represent two different species under the genus “Picea”, observed in the first Chinese data set
798 (CNi).

799 We derived plot-level abundance information in terms of species abundance matrices. Each
800 species abundance matrix consisted of the number of individuals by species (column vectors)
801 within individual sample plots (row vectors). In addition, key plot-level information was also
802 added to the matrices, including plot ID, data set name, plot coordinates, the year of measurement,
803 and basal area, i.e. the total cross-sectional areas (m^2) of living trees per one hectare of ground
804 area.

805 Tree genera were assigned to a plant family using a plant taxonomy lookup table generated
806 by Will Cornwell (hosted on Github https://github.com/traitecoevo/taxonlookup), which uses the
807 accepted taxonomy from “The Plant List.” The majority (96.5%) of genera from the GFBi species
808 were successfully matched to family; for those that could not be assigned, we manually checked
809 the GFBi genus and species against synonyms from The Plant List. Of the remaining 1,038
810 mismatches, an additional 440 were assigned to family either by updating older genera and species
811 names with their more recent synonyms or else by correcting obvious misspellings. The remaining
812 598 entries that could not be matched to family were excluded from analysis.

813 We used a taxonomically-informed approach to assign symbiotic states to plant species
814 from the GFBi. Plant species were assigned to one of 5 symbiotic guilds – ectomycorrhizal (EM),
815 arbuscular mycorrhizal (AM), ericoid mycorrhizal (ErM), weakly AM or non-mycorrhizal
816 (AMNM), or N-fixer (Table S1). Although we did not model the relative abundance of ErM trees,
817 due to their rarity, we have included a map of their relative abundance from our grid (Figure S1).
818 We also include as a supplementary file the full species list, which includes columns used to assign
819 species to guild. In addition, we include here a list of families and genera assigned to all guilds

except AM (Tables S2-5) with notes for cases of species from individual genera that were either assigned to two guilds simultaneously (e.g., *Alnus* is an N-fixer and EM) or where species from individual genera were split between two different guilds (e.g., some *Pisonia* sp. are weakly AM and some are EM). An AM summary table is excluded for length considerations—the same information is available in the Supplementary File "SymbioticGuildAssignment.csv".

The taxonomy of species in our inventory was compared with recently published literature on the evolutionary history of mycorrhizal symbiosis[7,33,34] and N-fixation[35-38]. Most species symbiotic status could be reliably assigned at the genus (e.g. *Dicymbe*) or family level (e.g. Pinaceae). For the few groups where status was unreliable or variable within a genus (e.g. *Pisonia*) we conducted additional literature searches.

We assigned species to the EM category in three stages. First, at the family level (e.g., Pinaceae); next, as the genus level (e.g., Dicymbe); and finally, using literature searches for unclear genera. For example, for the genus *Pisonia*, some species are AM and others are EM. We used a published list from Hayward & Hynson (2014)[39] to sort species into the appropriate guild. For the genus *Acacia*, we followed Brundrett (2017)[7] in assuming that only endemic Australian species associate with EM, while all others are AM (we sorted *Acacia* species according to provenance using http://worldwidewattle.com/).

The AMNM category lumped together all genera of terrestrial, non-epiphytic plants that either lack arbuscular mycorrhizal fungi (AMF), or have low or inconsistent records of AMF colonization of roots. For example, although there are some published records of AMF colonization in the roots of Proteaceae, these records are inconsistent, and colonization is generally low. Further, as Proteaceae are associated with a non-mycorrhizal root morphology (the "cluster" or "proteoid root system") that allows them to access otherwise unavailable forms of soil

nutrients[40], we placed the entire family within AMNM. The family Urticaceae, which we also characterized as AMNM, was somewhat problematic – early-successional species from tropical forests, such as those in the genus *Cecropia*, have records of both low and absent AMF colonization[41]. Our approach was to use the most broadly inclusive AMNM categorization.

N-fixer status was assigned at the genus level, using previously compiled databases of global symbiotic N_2-fixation[35-38]. Given that symbiotic N_2-fixation with rhizobial or *Frankia* bacteria has only evolved in four orders (Rosales, Cucurbitales, Fabales and Fagales)[42], all species outside of this nitrogen-fixing clade were assigned non-fixing status. Some species could not be assigned a N-fixer status because they were typed to a higher taxonomic level (e.g. family) that is ambiguous from a N-fixer status perspective. We recorded when our assignment of N-fixer status was based on phylogenetic criteria but where symbiotic N-fixation is evolutionarily labile. Since these cases are more likely to be misassigned we excluded them from the N-fixation category. The N-fixer group contains species that are colonized by AMF (e.g., most genera from Leguminosae) and others that are colonized by ectomycorrhizal fungi (e.g., *Alnus* sp.).

Most plant species form AM symbiosis, which is the basal symbiotic state to the later derived EM and N-fixing symbioses. Further, many EM and N-fixing plants maintain the ability to form AM symbiosis. Thus, a tree species is most likely AM if it does not form associations with another symbiotic guild (or forgoes root symbiosis entirely), as evidenced by their inclusion in exhaustive databases of plant symbiotic state[7,33-38,41]. In keeping with other large-scale studies in the field (e.g. [34]), we assigned tree species from the GFBi database to an AM-exclusive state if they belonged to taxa that were not matched to EM, ErM, non-or-weakly mycorrhizal or N-fixer symbioses. Thus, the AM and N-fixer groups in our dataset are non-overlapping despite the fact that most N-fixers also associate with AM fungi.

The proportions of tree basal area and tree individuals were aggregated to a 1' by 1' degree grid by taking the weighted average of the plot-level proportions (Table S6). This resulted in a total of 2,768 grid cells, each with a score for the proportional abundance of EM, AM, N-fixer, ErM, and AMNM trees. We calculated two measures of relative abundance for each symbiotic guild: proportion of tree stems and proportion of tree basal area. Because the measurements are highly correlated with one another (Figure S2) we chose to model only proportion of total tree basal area, which should scale more approximately to proportion of tree biomass as it accounts for differences in size among individual stems. Additionally, we quantified variability among plots within each grid cell by calculating the weighted standard deviation across the grid (Supplemental Information, Figure S3-4).

To identify the key factors structuring symbiotic distributions we assembled 70 global predictor layers: 19 climatic (annual, monthly, and quarterly temperature and precipitation variables), 14 soil chemical (total soil N density, microbial N, C:N ratios and soil P fractions, pH, cation exchange capacity), 5 soil physical (soil texture and bulk density), 26 vegetative indices (leaf area index, total stem density, enhanced vegetation index means and variances), and 5 topographic variables (elevation, hillshade) (Table S7). Because decomposition is the dominant process by which soil nutrients become available to plants, we generated 5 additional layers that estimate the climatic control of decomposition. We parameterized decomposition coefficients according to the Yasso07 model[20,43] using the following equation:

$$k = \mathrm{Exp}(0.095 T_i - 0.00014\, T_i^2)\,(1-\mathrm{Exp}[\,-1.21\, P_i]), \qquad (1)$$

where P_i and T_i are precipitation and mean temperature, either quarterly or annually, and the constants 0.0095 ($=\beta_1$) $=$0.00014 ($=\beta_2$), and -1.21 ($=\gamma$) are parameters fit using a previous global study of leaf litter mass-loss[20]. Although local decomposition rates can vary significantly based on

889 litter quality or microbial community composition[44], climate is the primary control at the global
890 scale[20]. Decomposition coefficients describe how fast different chemical pools of leaf litter lose
891 mass over time relative to a parameter, α, that accounts for leaf-chemistry. Decomposition
892 coefficients (k) with values of 0.5 and 2 indicate a halving and doubling of decomposition rates
893 relative to α, respectively (Supplemental Information, Figure S5).

894 We implemented the random forest algorithm using the "randomForest" packaged in R.
895 Random forest models average over multiple regression trees, each of which uses a random subset
896 of all the model variables to predict a response. We first determined the influence and relationship
897 of all 75 predictor layers on forest symbiotic state and then optimized our models using a stepwise
898 reduction in variables, from least- to most-important. Variable importance was measured in two
899 ways: Inc Node Purity and %IncMSE (with values reported in each panel of Figure 2). The inc
900 node purity of variable x considers the decrease in the residual sum of squares that results from
901 splitting regression trees using variable x. %IncMSE (mean square error) quantifies the increase
902 in model error as a result of randomly shuffling the order of values in the vector x. We chose to
903 rank variables according to inc node purity because we found that higher inc node purities were
904 associated with larger effect sizes, whereas larger %IncMSE were associated with more linear
905 responses of smaller effect. Whereas our inspection of partial feature contributions is derived from
906 univariate random forest models, we additionally ran multivariate random forests the predict the
907 proportional abundance of EM, AM, and N-fixer trees for each pixel. The multivariate models
908 were run using 50-regression trees each, with the unique set of the best 4 predictor variables for
909 each symbiotic guild in the univariate models (Table S7, Figure 2). Despite strong negative
910 correlations between the proportions of EM and AM basal area (Figure S22), the results from
911 multivariate and univariate random forests are strongly correlated with one another (Figure S23).

912 Using model selection based on eliminating variables with low Inc Node Purity, we
913 removed most soil nutrient, vegetative, and topographic variables from our models (Figure S6-7).
914 Our final models include the remaining 34 predictor layers with climate, decomposition, and
915 certain soil physical and chemical information (Figure S8). To determine the parsimony of our
916 models, we compared the coefficient of determination in models run with a stepwise reduction in
917 the number of variables (starting with those with the lowest Inc Node Purity). Based on
918 performance of the ratio of coefficient of determination in models with 4 vs 34 variables, we
919 determined that the 4 most important variables accounted for >85% of the explained variability
920 (Figure S9). We also compared model performance visually with plots of actual vs predicted
921 proportions of each tree symbiotic guild among continents and geographic subregions (Figure
922 S10). We used the "forestFloor" packaged in R to plot the partial variable response of tree
923 symbiotic guilds to each predictor variable (Figure 2ABC, see Figure S19-21 for partial plots of
924 the partial feature contributions of all 34 variables).
925 In order to test the sensitivity of model performance and predictions, we performed cross
926 validation in R using the "rfUtilities" package[24]. K-fold cross validation tests the sensitivity of
927 model predictions to losing random subsets from the training data. For EM, AM, and N-fixer
928 models we ran 99 iterations that withheld 10% of the model training data. We assessed the drop in
929 model performance in the 99 iterations by manually calculating the coefficient of determination,
930 which uses the following formula: $1 - \Sigma (\text{actual \% basal area} - \text{predicted \% basal area})^2 / \Sigma (\text{actual \% basal area} - \text{mean actual \% basal area})^2$. For all symbiotic guilds, withholding 10% of
931 the training data resulted in a mean loss in variance explained of less than 1% (Figure S11). This
932 shows that our training data has sufficient redundancy to ensure that our model conclusions are
933 robust. Similarly, to determine whether our random forest models would make similar predictions
934

935 if data were equally distributed among continents, we rarefied our aggregated grid of symbiotic
936 states and predictor layers to an even depth. Specifically, we sub-sampled all continents – N.
937 America (including Central America and the Caribbean), S. America, Europe, Asia, and Oceania
938 – to match the number of grid-pixels from Africa (n=50). This is a much more aggressive reduction
939 of training data than is typically used in K-fold cross validations, as it involves dropping ~90% of
940 training data rather than retaining the same amount. We performed 99 iterations of rarefaction each
941 for the three symbiotic guilds. On average, models run with the rarefied data explained about 10%
942 less variance over the full training data (the entire predictor / response grid) than did models run
943 with all of the training data (Figure S12-13).

944 To avoid projecting our random forest models outside the ranges of their training data (e.g.,
945 grid cells with higher mean annual temperatures than the maximum used to fit the models), we
946 subset a global grid of predictor layers depending on whether (1) the grid cell fell within the top
947 60% of land surface with respect to tree stem density[11] and either (2) fell within the univariate
948 distribution of all the predictor layers from our training data and/or (3) fell within an 8-dimensional
949 hypervolume defined by the unique set of the 4-best predictors of the relative abundance of each
950 guild (Figure S14). We then projected our models across only those grid cells that met these
951 criteria, which constitutes 46% of the global land surface and 88% of global tree stems (Figure 1;
952 Figure S15). Model projections were made at two resolutions: both 1 by 1 degree and 0.5 by 0.5
953 degree resolution (Figure 4). While model validation indicates that our projections are robust,
954 additional ground truthing of predictions to identify any discrepancies would be incredibly
955 valuable. If such discrepancies exist they can help fine tune climate-symbiosis models, or identify
956 areas where climate might favour invasion by symbioses that have not yet evolved or dispersed to
957 a particular biogeographic region.

We used the following equation to estimate the % of global tree stems that belong to each tree symbiotic guild: Σ_i (predicted proportion of trees of guild *g* in pixel *i*) x (total number of tree stems in pixel *i*) / Σ_i (total number of tree stems in pixel i). The proportion of tree stems and the proportion of tree basal area in each guild are highly correlated throughout the training data (Figure S4). The figures cited in the main text for each guild were calculated using model projections across all pixels, even those that did not meet the criteria for model projection because they fell outside the multivariate distribution of the predictor layers or had insufficient stem density. However, our estimates for the global % of trees occupied by each tree symbiotic guild change by <1% when using only those pixels that met our criteria for model projection.

In the main manuscript we state that sharp transitions between dominant symbiotic states with climate variables could lead to declines in EM trees, particularly in southern boreal forests. To determine this, we projected our random forest models for each symbiotic guild using climate change projections over our 19 bioclimatic variables (Table S7), including the decomposition coefficients that use temperature and precipitation values. Specifically, we considered the 2070 scenario with a relative concentration pathway (RCP) of 8.5 (W/m^2), which predicts an increase of greenhouse gas emissions throughout the 21st century[45]. We plot difference in the proportion of forest basal area between the projections for 2070 and those using current climate data (Table S7, Figure S24). We qualify this prediction with the note that vegetative changes to forests are constrained by rates of mortality, recruitment, and growth.

After training and cross-validating our models with GFBi data exclusively, we additionally tested whether our models accurately predicted the symbiotic state of Eurasian forests previously published by Schepaschenko et al. (2017)[46]. We assigned symbiotic status to all trees in Schepaschenko et al. (2017) and aggregated plot level data to a 1 by 1 degree grid using the same

methods as with the GFBi dataset (Figure S25). We found that, on average, our models predicted the symbiotic state in the regional dataset within 13.6% of the value of this other dataset (Figure S26). For projected maps in Figure 4abc, we included the Schepaschenko et al. (2017) data with the GFBi training data to increase geographic coverage throughout Eurasia.

Methods References

31 Liang, J. *et al.* Positive biodiversity-productivity relationship predominant in global forests. *Science* **354**, aaf8957 (2016).

32 Chamberlain, S. A. & Szöcs, E. taxize: taxonomic search and retrieval in R. *F1000Research* **2** (2013).

33 Brundrett, M. C. & Tedersoo, L. Evolutionary history of mycorrhizal symbioses and global host plant diversity. *New Phytol.* (2018).

34 Brundrett, M. C. Mycorrhizal associations and other means of nutrition of vascular plants: understanding the global diversity of host plants by resolving conflicting information and developing reliable means of diagnosis. *Plant and Soil* **320**, 37-77, doi:10.1007/s11104-008-9877-9 (2009).

35 Werner, G. D., Cornwell, W. K., Sprent, J. I., Kattge, J. & Kiers, E. T. A single evolutionary innovation drives the deep evolution of symbiotic N 2-fixation in angiosperms. *Nature Communications* **5**, 4087 (2014).

36 Werner, G. D., Cornwell, W. K., Cornelissen, J. H. & Kiers, E. T. Evolutionary signals of symbiotic persistence in the legume–rhizobia mutualism. *Proceedings of the National Academy of Sciences* **112**, 10262-10269 (2015).

37 Afkhami, M. E. *et al.* Symbioses with nitrogen-fixing bacteria: nodulation and phylogenetic data across legume genera. *Ecology* **99**, 502-502 (2018).

38 Tedersoo, L. *et al.* Global database of plants with root-symbiotic nitrogen fixation: Nod DB. *Journal of Vegetation Science* (2018).

39 Hayward, J. & Hynson, N. A. New evidence of ectomycorrhizal fungi in the Hawaiian Islands associated with the endemic host Pisonia sandwicensis (Nyctaginaceae). *Fungal Ecol* **12**, 62-69 (2014).

40 Lambers, H., Martinoia, E. & Renton, M. Plant adaptations to severely phosphorus-impoverished soils. *Current opinion in plant biology* **25**, 23-31 (2015).

41 Wang, B. & Qiu, Y.-L. Phylogenetic distribution and evolution of mycorrhizas in land plants. *Mycorrhiza* **16**, 299-363 (2006).

42 Soltis, D. E. *et al.* Chloroplast gene sequence data suggest a single origin of the predisposition for symbiotic nitrogen fixation in angiosperms. *Proceedings of the National Academy of Sciences* **92**, 2647-2651 (1995).

43 Palosuo, T., Liski, J., Trofymow, J. & Titus, B. Litter decomposition affected by climate and litter quality—testing the Yasso model with litterbag data from the Canadian intersite decomposition experiment. *Ecological Modelling* **189**, 183-198 (2005).

44 Bradford, M. A. *et al.* Climate fails to predict wood decomposition at regional scales. *Nature Climate Change* **4**, 625 (2014).
45 Allen, M. R. *et al.* IPCC fifth assessment synthesis report-climate change 2014 synthesis report. (2014).
46 Schepaschenko, D. *et al.* A dataset of forest biomass structure for Eurasia. *Scientific data* **4**, 170070 (2017).

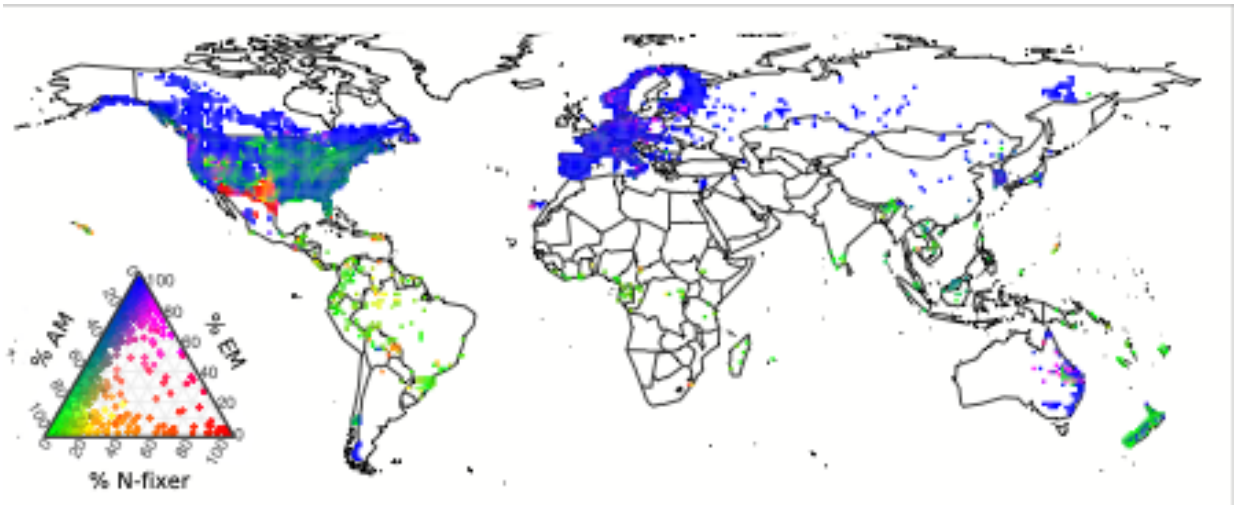

Fig. 1. The global map has n = 2,768 grid cells at a resolution of 1° × 1° latitude and longitude. Cells are coloured in the red, green and blue spectrum according to the percentage of total tree basal area occupied by N-fixer, arbuscular mycorrhizal (AM) and ectomycorrhizal (EM) tree symbiotic guilds, as indicated by the ternary plot.

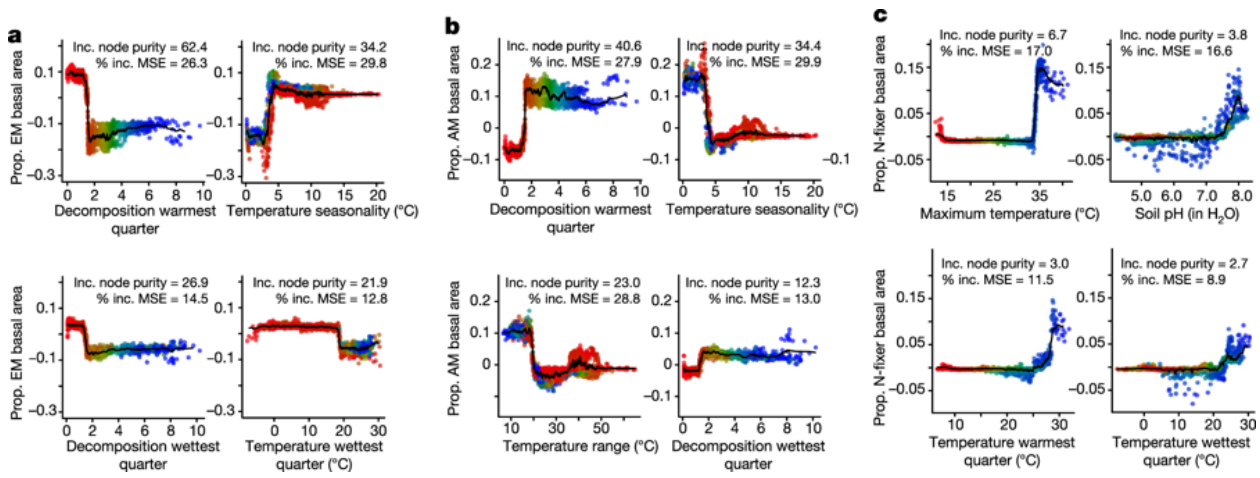

Fig. 2. a–c, Partial feature contributions of different environmental variables to forest symbiotic state. Each row plots the shape of the contribution of the four most-important predictors of the proportion of tree basal area that belongs to the ectomycorrhizal (a), arbuscular mycorrhizal (b) and N-fixer (c) symbiotic guilds (n = 2,768). Variables are listed in declining importance from left to right, as determined by the increase in node purity (inc. node purity), and with points coloured with a red to green to blue gradient according to their position on the x axis of the most-important variable (left-most panels for each guild), allowing cross-visualization between predictors. Each panel lists two measures of variable importance; inc. node purity (used for sorting) and percentage increase in mean square error (% inc. MSE) (see Supplementary Information). The abundance of each type of symbiont transitions sharply along climatic gradients, which suggests that sites near the threshold are particularly vulnerable to switching their dominant symbiont guild as climate changes. Warmest and wettest quarter, the warmest and wettest quarters of the year, respectively.

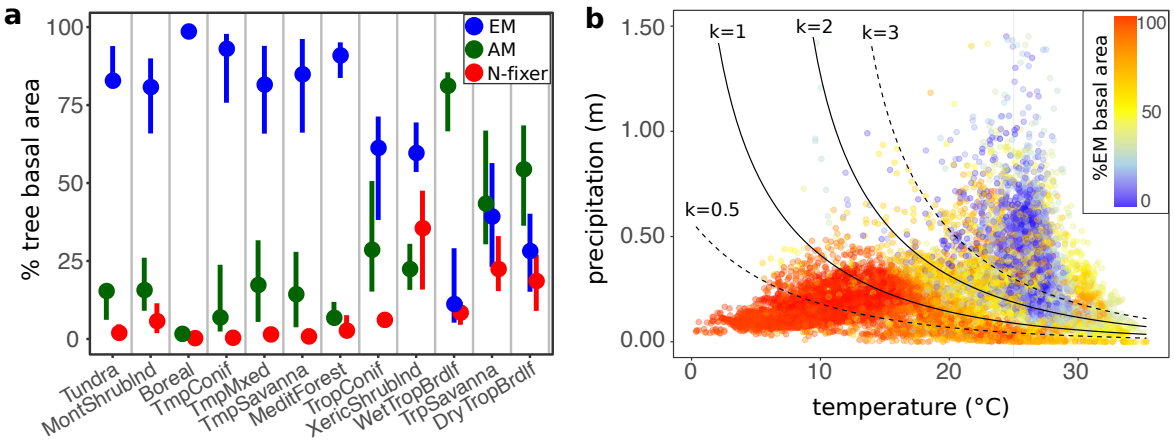

Fig. 3. a, Biome level summaries of the median ± 1 quartile of the predicted percentage of tree basal area per biome for ectomycorrhizal, arbuscular mycorrhizal and N-fixer symbiotic guilds (n = 100 random samples per biome). b, The dependency of decomposition coefficients (k, solid and dotted lines; in the region between the solid lines, the model transitions abruptly between dominant symbiotic status) on temperature and precipitation during the warmest quarter with respect to predicted dominance of mycorrhizal symbiosis. The transition from arbuscular mycorrhizal forests to ectomycorrhizal forests between k = 1 and k = 2 is abrupt, which is consistent with positive feedback between climatic and biological controls of decomposition.

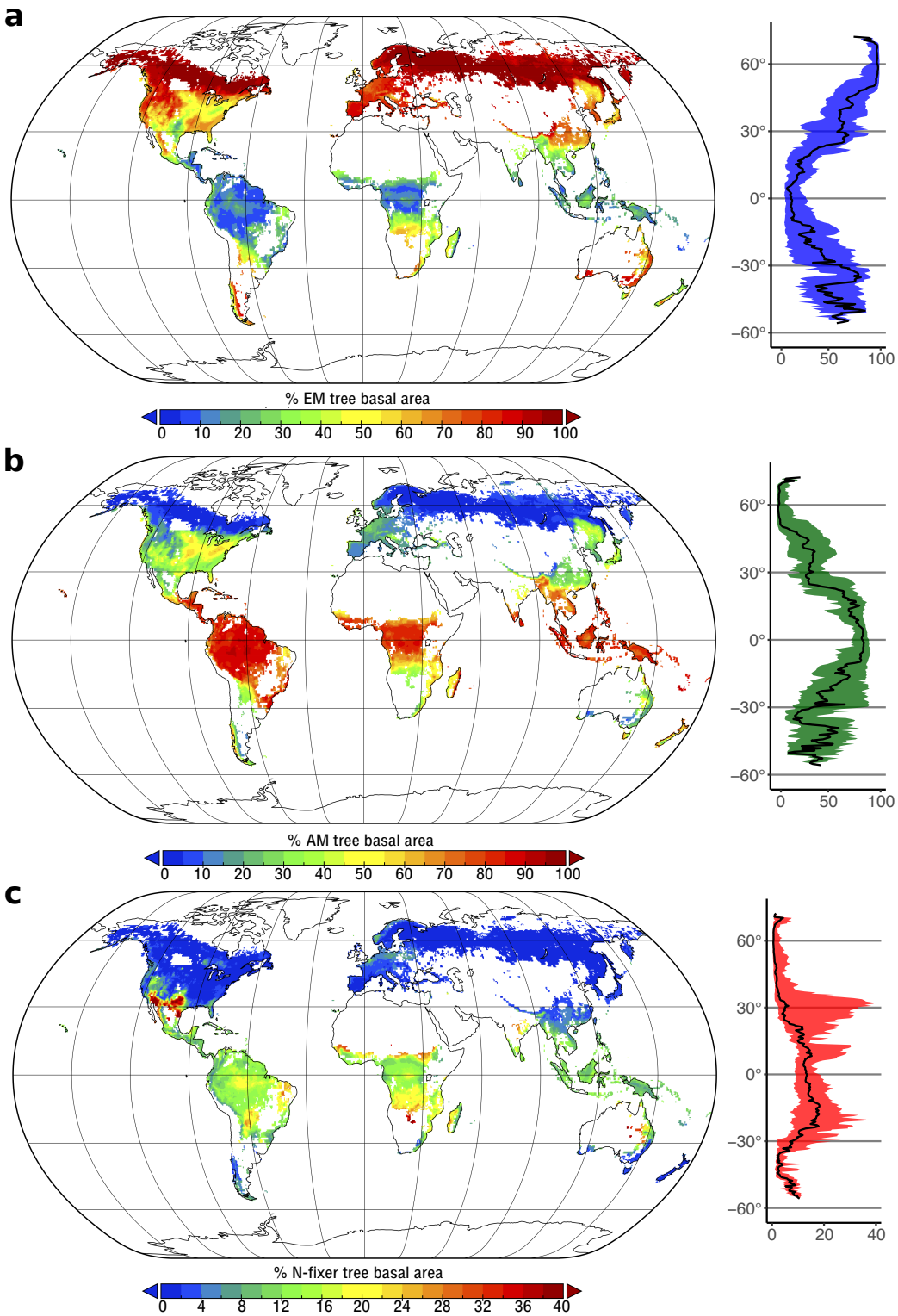

1066

1067 Fig. 4. a–c, Maps (left) and latitudinal gradients (right; solid line indicates median; coloured ribbon

1068 spans the range between the 5% and 95% quantiles) of the percentage of tree basal area for

1069 ectomycorrhizal (a), arbuscular mycorrhizal (b) and N-fixer (c) symbiotic guilds. All projections

1070 are displayed on a 0.5°-by-0.5° latitude and longitude scale. n = 28,454 grid cells.